Effect of Copolymer Composition on the Phase Behavior of Mixtures of Poly(ethylene-*co*-methyl acrylate) with Propane and Chlorodifluoromethane

Melchior A. Meilchen, Bruce M. Hasch, and Mark A. McHugh*

Department of Chemical Engineering, Johns Hopkins University, Baltimore, Maryland 21218

Received March 7, 1991; Revised Manuscript Received May 2, 1991

ABSTRACT: Experimental data are presented on the high-pressure phase behavior and fractionation of polyethylene, poly(ethylene-*co*-methyl acrylate) (90 mol %/10 mol %), poly(ethylene-*co*-methyl acrylate) (64 mol %/36 mol %), and poly(methyl acrylate), with propane and chlorodifluoromethane. Cloud-point curves are obtained at temperatures ranging from 50 to 160 °C and pressures to 2000 bar. As the acrylate content in the backbone of the copolymer increases, chlorodifluoromethane becomes a better solvent for the copolymer probably because it hydrogen bonds to the basic acrylate group. The effect of polydispersity on the phase behavior is secondary to the effect of acrylate content of the polymer. The Sanchez-Lacombe equation of state, with two mixture parameters, is used to model the cloud-point curves. The characteristic parameters for the copolymers are calculated by assuming that the copolymer is a statistically random mixture of homopolymers. No apparent trends are observed in the mixture parameters as a function of copolymer composition.

Introduction

To ensure the efficient free-radical polymerization of polyethylene and ethylene-based copolymers, it is necessary to operate in the single-phase region. Typical operating conditions are temperatures ranging from 100 to 200 °C and pressures as high as 2000 bar.[1] The elevated pressures are needed to solubilize the high molecular weight polymers that are formed in ethylene. When copolymers are formed, the pressure needed to maintain a single phase can increase depending on the type of comonomer used in the process. For example, Rätzsch and co-workers[2-4] showed that at a given temperature the cloud-point pressure for poly(ethylene-*co*-vinyl acetate) (EVA) dissolved in ethylene increases by as much as 100 bar as the vinyl acetate content in the backbone of the copolymer increases from 0 to 20 mol %. Interestingly, temperature had only a minor effect on the cloud-point pressure in the range of 120–200 °C. These studies were performed with copolymers with number-average molecular weights ranging from 14 000 to 20 000 and polydispersities in the range of 1.3–6.1. Rätzsch and co-workers also reported that fractionating the parent EVA copolymers by using a liquid antisolvent technique yields fractions that differ only in molecular weight and not in the chemical composition of the copolymer.

In this paper we present the results from an experimental investigation of the effect of methyl acrylate (MA) content on the cloud-point curves of poly(ethylene-*co*-methyl acrylate) in propane and chlorodifluoromethane (F22). The experimental data are modeled with the Sanchez–Lacombe equation of state.[5] The four polymers studied include two homopolymers, polyethylene and poly(methyl acrylate), and two copolymers, one with 90 mol % ethylene (or, equivalently, 75 wt %) and the other with 64 mol % ethylene (or, equivalently, 37 wt %). In addition to phase behavior information, we present data on the fractionation of the four polymers using supercritical propane and F22. Supercritical fluid fractionation is a reasonably rapid technique that results in gram-size samples of narrow molecular weight distributions, in contrast to liquid antisolvent fractionation. In certain instances cloud-point curves are obtained with the parent polymer as well as with fractionated polymer. Table I lists the properties of the two solvents used in this study, propane and F22, which were chosen since they have similar critical temperatures and pressures but very different densities and polarities. F22, which hydrogen bonds to basic molecules, such as methyl acrylate, but does not hydrogen bond to itself, should be a better solvent for the high acrylate content polymers.[6,7] We chose to work with propane rather than ethylene since the double bond in ethylene results in a quadrupolar contribution to the ethylene–copolymer attractive potential, which can complicate the interpretation of the phase-behavior differences between the copolymer dissolved in ethylene versus F22.

Table I
Properties of Propane and Chlorodifluoromethane[28]

component	T_c, °C	P_c, bar	crit density, g/mL	dielectric const, D
C_3H_8	96.7	42.5	0.217	0.0
$CHClF_2$	96.2	49.7	0.522	1.4

The cloud-point behavior for the polymer–propane and polymer–F22 systems obtained in this study can be described by use of two classes of binary, pressure–temperature (P–T) diagrams, which originate from P–T diagrams for small molecule systems. The first type of schematic P–T diagram for small molecule mixtures is shown in Figure 1A, where the vapor–liquid equilibrium curves for two pure components end in their respective critical points, C_1 and C_2.[8,9] The dashed lines in Figure 1A are critical mixture curves that represent either liquid–vapor or liquid–liquid critical points for mixtures of different composition. Figure 1B shows the schematic P–T diagram for a pseudobinary polymer–solvent mixture, which corresponds to the behavior shown in Figure 1A. Since a pure polymer does not have a critical point or vapor pressure curve, the high-temperature portion of the critical mixture curve does not exist. The branch of the critical mixture curve that is observed is termed a lower critical solution temperature (LCST) curve since the solution merges into a single phase as the temperature is decreased at a constant pressure. Also, typically, the liquid–liquid–vapor (LLV) line superposes on the vapor pressure curve of the pure solvent. Numerous binary polymer–solvent mixtures exhibit the phase behavior depicted in Figure 1B.[10-13]

0024-9297/91/2224-4874$02.50/0

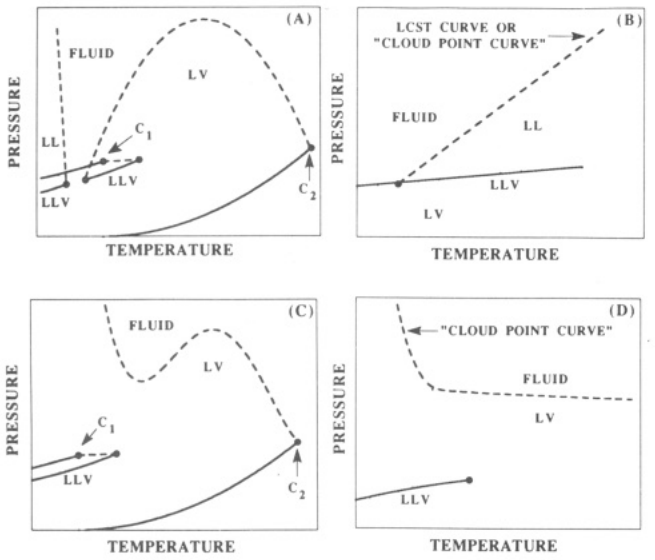

Figure 1. Pressure–temperature diagram for a binary mixture. C_1 and C_2, critical points of components 1 and 2, respectively; LLV, liquid$_1$ + liquid$_2$ + vapor. Panels A and C represent small molecule systems and panels B and D represent polymer systems.

Figure 1C shows the other type of P–T diagram that can occur with small molecule mixtures if the disparity in the size and/or the intermolecular potentials of the mixture components becomes large. In this instance, the low-temperature liquid–liquid (LL) to fluid transition line shown in Figure 1A has merged with the critical mixture curve. Notice that the critical mixture curve does not intersect the LLV line, rather it shows a minimum in pressure and goes to very high pressures as the temperature is lowered. Figure 1D shows how Figure 1C is transformed for polymer–solvent systems. If the polymer exhibits any significant degree of crystallinity, it is possible for the crystallization boundary to intrude on the fluid-phase portion of the phase diagram and obscure the change in slope of the cloud-point curve. Therefore, at conditions near the crystallization temperature of the polymer, fluid → liquid + vapor transitions become fluid → fluid + solid transitions.

One final difference between schematic P–T diagrams for mixtures of small molecules (Figure 1A and 1C) and polymer–solvent mixtures (Figure 1B and 1D) is that a cloud-point curve at a fixed concentration of ~5 wt % polymer is reasonably close to the true LCST curve.[10,14] Hence, constant-concentration, cloud-point data are reported here instead of LCST data.

Experimental Section

Two types of experiments are reported here. The fractionation is performed using a dynamic flow technique[15,16] and the cloud-point curves are obtained with a high-pressure, variable-volume view cell.[13,17] These techniques are briefly described.

Each of the polymers is fractionated using the dynamic flow apparatus capable of operating to 170 °C and 600 bar shown in Figure 2. A measured amount of polymer, typically 7 g, is charged to each extraction column (1.8 cm i.d. × 30 cm long). The columns are packed carefully to ensure proper contact between the supercritical fluid and the polymer, to maintain the polymer in the columns even if the polymer liquefies at operating conditions, and to allow for sufficient room for the liquid polymer solution to expand as the supercritical fluid dissolves in it. The column is packed first with glass wool in the bottom, then a ~1-cm layer of 4-mm-o.d. glass beads is placed into the column, and then a ~2.5-cm layer of polymer is added. This sequence is repeated until the column is filled. Glass wool is also placed at the top of the column to help remove any polymer entrained in the flowing gas stream. Liquid propane or F22 is supplied to a diaphragm compressor (Superpressure, Model J46-14025-1) and delivered

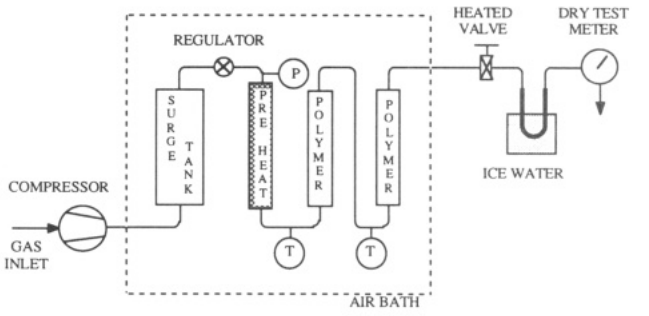

Figure 2. Schematic diagram of the high-pressure flow apparatus used to fractionate polymers.

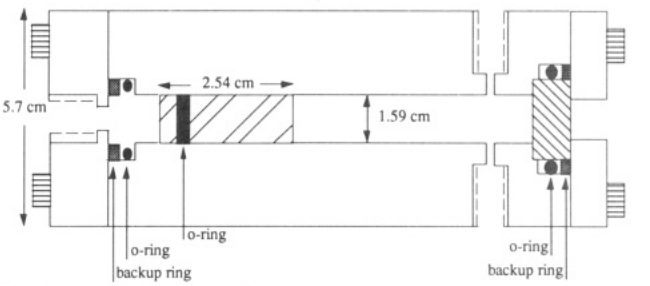

Figure 3. Schematic diagram of the variable-volume, high-pressure cell used to obtain cloud-point data.

to a surge tank. The flow rate through the columns is typically maintained in the range of 2.5–8.5 ± 1.4 L/min (STP) (~8.0 ± 4.0 g/min). The system pressure is controlled to within ±5.0 bar by a pressure reducing regulator (Tescom, Model 26-1000) between the columns and the surge tank, which is normally maintained 200 bar greater than the column pressure. A heated valve (HIP Inc., Model 30-12HF4-HT) at the outlet to the columns restricts the gas flow sufficiently to allow for control of the flow rate. Before entering the extraction columns, the gas flows through a preheater to reach thermal equilibrium with the air bath. The temperature of the gas is maintained to within ± 1.0 °C as measured with two platinum resistance thermal devices located at the entrances to the first and second extraction columns.

At a fixed temperature, the pressure of the columns is set and the gas is allowed to flow through the columns for typically 30 min. The loaded gas phase exiting the column is expanded through a heated pressure let-down valve where polymer precipitates from the expanded low-pressure gas into a preweighed U-tube situated in an ice–water bath. Glass-wool filters at the exit of the U-tube trap any fine mist entrained in the gas. The gas is routed to a dry-test meter (Singer American Meter Division, Model DTM-200) to monitor the total volume passed through the extractors. The operating pressure is then raised incrementally to obtain the next polymer fraction. The polymer samples in the U-tubes are weighed and subsequently analyzed by gel permeation chromatography. As noted in the tables, some of the samples were analyzed with use of polyethylene standards and the others were analyzed with use of polystyrene standards. The copolymer samples are also analyzed for acrylate content by NMR and FTIR, and the percent crystallinity in the high ethylene content polymers is determined to within ±5% by DSC.

Figure 3 shows a schematic diagram of the high-pressure, variable-volume view cells used to obtain cloud-point data. For pressures of less than 1000 bar, a cell constructed of 316 stainless steel was used (6.4 cm o.d. × 1.9 cm i.d., ~40-cm^3 working volume, fitted with a 3.8 cm o.d. × 1.91 cm thick sapphire window). For pressures above 1000 bar, a cell constructed of a high nickel content steel was used (Nitronic 50, 5.7 cm o.d. × 1.59 cm i.d., ~22-cm^3 working volume, fitted with a 1.9 cm o.d. × 1.3 cm thick sapphire window).[18] Except for the view cells, all other aspects of the experimental apparatus and techniques are the same. The cell, which is initially loaded with a measured amount of polymer to within ±0.002 g, is purged three or more times at room temperature with either propane or F22 at ~3–6 bar to remove any entrapped air. The gas of interest is then transferred into the cell gravimetrically to within ±0.002 by use of a high-pressure

Table II
Fractionation of Poly(methyl acrylate) Using Chlorodifluoromethane at 138 °C and at Pressures Ranging from 130 to 300 Bar[a]

fractn	P, bar	$\sum w$,[b] wt %	M_n	M_w	M_w/M_n
1–4[c]	178	1.7			
5	205	2.3	900	20 100	bimodal
6	233	16.7	156 200	349 800	2.2
7	231	24.4	200 600	440 900	2.2
8	245	41.5			
9	258	67.2			
10	274	70.5	725 400	1 142 600	2.0
11	299	72.6	884 200	1 767 900	1.6

[a] Molecular weight analysis is based on polystyrene standards. [b] $\sum w$ is the cumulative weight percent polymer removed from the column. [c] An insufficient amount of material was recovered with fractions 1–4 for analysis.

bomb. The solution can be compressed to the desired operating pressure by displacing a movable piston fitted within the cell by using water pressurized with a high-pressure generator (HIP Inc., Model 37-5.75-60). The pressure of the polymer solution is determined by measuring the pressure of the water with a Heise gauge accurate to within ±2.8 bar for pressures greater than 1000 bar and ±1.4 bar for pressures less than 1000 bar. A small correction is added for the pressure needed to move the piston (~1.0 bar). The temperature of the cell, which is measured to within ±0.2 °C with a platinum resistance device connected to a digital multimeter, is also maintained to within ±0.2 °C. The contents of the cell are mixed by a glass-encased stir bar activated by a magnet located below the cell.

At a fixed temperature the mixture in the cell is compressed to a single phase. The pressure is then slowly decreased until it begins to get cloudy. Two methods are used to determine the reported cloud-point pressure. In one, the polymer–gas mixture in the cell is projected onto a video monitor with a borescope (Olympus Corp., Model D100-048-000-90) placed against the sapphire window and connected to a video camera. The cloud-point pressure is defined as the point at which the mixture becomes so opaque that it is no longer possible to see the stir bar in the solution. This visual observation was checked against the output from a 10-mW laser (Melles Griot, Model 05-LHP-151), which was directed into the cell and reflected off a small mirror. In this instance the cloud-point pressure is defined as the point at which a 90% decrease in laser light is obtained. The cloud points obtained with both techniques are within the reproducibility reported for the cloud-point pressure, which is typically ±5 bar. Cloud-point determinations are done at constant polymer concentration, which in this study is maintained between 4.5 and 5.5 wt %.

Materials. The polymers were kindly donated by Du Pont. Propane (CP grade, 99.0% minimum purity) was obtained from Linde Corp. and chlorodifluoromethane (99.8% minimum purity) was obtained from Matheson Gas Products.

Results

Fractionation. In this phase of the study, the parent polymers were fractionated with supercritical propane or F22. No attempt was made to optimize the fractionation; rather the objective was to obtain gram-size samples of reasonably narrow molecular weight distributions for the phase-behavior studies. Table II shows the results from the fractionation of poly(methyl acrylate) (PMA) using F22 at 138 °C, approximately 42 °C above its critical temperature. The polydispersity of the fractions that are analyzed is near 2.0. Although 11 total fractions were obtained, the first four represent less than 2 wt % of the initial charge of polymer placed in the columns and were not analyzed, and we were not able to analyze the parent polymer due to experimental difficulties with the GPC. At about 230 bar, the solubility of the lower molecular weight fractions in the parent polymer increases quite substantially in F22. Notice that fraction 6 was obtained at a slightly higher pressure than fraction 7, but it has a slightly lower average molecular weight. In this instance such a large amount of polymer was extracted from the column that the U-tube that held fraction 6 had to be changed during sampling and the average pressure decreased slightly while the rest of the sample, now designated fraction 7, was recovered. The molecular weight of fraction 7 indicates that although the pressure used to obtain fraction 6 is high enough to extract high molecular weight polymer the lower molecular weight oligomers come out first. Notice also that more than 25 wt % of the highest molecular weight material remains in the column with the original charge. This observation will be important when we discuss the cloud-point behavior of this polymer. Fractionation of PMA with propane is not feasible since it does not dissolve in propane to any great extent at temperatures to 140 °C and pressures to 500 bar.

Table III
Fractionation of Poly(ethylene-*co*-methyl acrylate) (64 mol %/36 mol %) Using Chlorodifluoromethane at 138 °C and at Pressures Ranging from 130 to 350 Bar

fractn	P, bar	$\sum w$,[a] wt %	M_n	M_w	M_w/M_n	MA,[b] mol %
		(A) Polyethylene Standards				
1	137	1.1	360	1 570	bimodal	39.8
2	240	40.5	16 700	34 400	2.1	36.2
3	274	69.5	81 100	152 000	1.9	35.5
4	280	89.6	91 800	137 000	1.5	35.0
5	346	100.0	219 000	350 000	1.6	35.1
parent			23 200	108 000	4.6	35.8
		(B) Polystyrene Standards				
1–2[c]	164	4.0				
3	193	10.9	13 600	16 300	1.2	
4	219	19.1	32 900	78 900	2.4	
5	247	65.1	50 400	63 500	1.3	
6	274	96.5	110 000	148 800	1.4	
7	303	100.0	338 000	454 900	1.4	
parent			48 300	122 400	2.6	35.8

[a] $\sum w$ is the cumulative weight percent polymer removed from the column. [b] Mole percent methyl acrylate in the copolymer. [c] An insufficient amount of material was recovered with fractions 1 and 2 for analysis.

Table III shows two sets of experimental results from the fractionation of poly(ethylene-*co*-methyl acrylate) (EMA) (64 mol %/36 mol %) again using F22 at 138 °C. Even though there is 64 mol % ethylene in the backbone of this copolymer, propane does not dissolve it to any great extent at pressures to 500 bar. The data in Table 3A show that the amount of polymer dissolved in F22 increases quite significantly at 240 bar. The chromatogram for fraction 1 was bimodal, indicating the presence of two different chemical species, possibly one copolymer rich in ethylene mixed with another copolymer rich in acrylate. It is also possible that this first fraction contained entrapped unreacted monomer. The methyl acrylate content in the copolymers removed in each fraction is essentially the same as that of the parent copolymer with the exception of fraction 1. Since the crystallinity of the parent copolymer was less than 5%, no attempt was made to determine the crystallinity of the fractions. Fractions 3–5 show that the polydispersity can be reduced to levels of 1.9 and below. In this case it is possible to remove all of the polymer from the columns because the molecular weight of the parent material was significantly lower than that of the previous poly(methyl acrylate) case shown in Table II. Comparing the results from the second experiment listed in Table 3B with those listed in Table 3A shows that the molecular weight distribution of the copolymer can be reduced to modest levels of 1.4 and lower if smaller pressure increments are taken between each pressure level. The tradeoff is that smaller pressure increments result in smaller sample sizes.

Table IV
Fractionation of Poly(ethylene-co-methyl acrylate) (90 mol %/10 mol %) Using Propane at 135 °C and at Pressures Ranging from 230 to 450 Bar[a]

fractn	P, bar	$\sum w$,[b] wt %	M_n	M_w	M_w/M_n	MA,[c] mol %	% crystallin
1–7[d]	247	2.4					
8	270	2.9	8 900	11 600	1.3		
9	293	3.4	10 700	14 000	1.3		
10	320	4.7	10 700	14 600	1.4		
11	338	6.4	13 200	18 100	1.4		
12	371	10.9	18 700	25 000	1.4		17.5
13	451	16.9[e]	20 100	28 500	1.4	9.5	
parent			17 000	75 400	4.4	9.8	17.3

[a] Molecular weight analysis is based on polyethylene standards. [b] $\sum w$ is the cumulative weight percent polymer removed from the column. [c] An insufficient amount of material was recovered with fractions 1–7 for analysis. [d] Mole percent methyl acrylate in the copolymer. [e] Estimated cumulative weight percent.

Table V
Fractionation of Polyethylene Using Propane at 135 °C and at Pressures Ranging from 100 to 610 Bar[a]

fractn	P, bar	$\sum w$,[b] wt %	M_n	M_v	M_w	M_w/M_n	% crystallin
1–7[c]	292	3.4					
8	324	4.6	3 000		5 900	1.9	
9–11[c]	391	9.7					
12	410	12.9	16 300		19 700	1.2	39.6
13	429	16.4		17 800			36.8
14	442	20.7	22 900		27 500	1.2	37.7
15	460	27.7					
16	482	40.8		30 200			
17–18[c]	495	57.7					
19	512	68.5	52 100		64 800	1.2	
20	523	78.6					
21	530	85.5	90 200		113 000	1.3	36.5
22	541	92.0					
23	551	97.7		115 000			35.0
24	609	100.0	167 000		389 000	2.3	36.6
parent			20 100		108 000	5.4	36.8

[a] Molecular weight analysis is based on polyethylene standards. M_v is the viscosity-average molecular weight. [b] $\sum w$ is the cumulative weight percent polymer removed from the column. [c] An insufficient amount of material was recovered with fractions 1–7, 9–11, 17, and 18 for analysis.

Table IV shows the results from the fractionation of 90 mol %/10 mol % EMA using propane at 135 °C. Fractionation of this high ethylene content copolymer in F22 is not feasible since its solubility in F22 is very small. Many features of this fractionation are similar to those of the previous 64 mol %/36 mol % EMA copolymer. For instance, the methyl acrylate content of fraction 13 is essentially equivalent to that found in the parent copolymer even though the polydispersity of this fraction is significantly lower than that of the parent. On the basis of this observation, and that the composition of the 64 mol %/36 mol % EMA copolymer did not vary with fractionation, we assume that the compositions of the other fractions in Table IV are very close to that of the parent copolymer. The polydispersities of the fractions listed in Table IV are very low since small pressure increments (~20 bar) are used between each pressure level. No attempt is made to fractionate the entire amount of copolymer charged to the columns since we collected enough material for our phase-behavior studies. It is interesting to note that the parent copolymer had a crystallinity of ~17.5% even though it consists of 10 mol % methyl acrylate. Although the polydispersity of fraction 12 is significantly lower than that of the parent, the percent crystallinity is virtually identical. The melting temperature was 86 °C for the parent copolymer as well as for the fractions.

Table V shows the results from a partial analysis of the fractionation of polyethylene using propane at 135 °C. Since F22 did not dissolve the 90 mol %/10 mol % EMA copolymer, no attempt was made to fractionate polyethylene with F22. In this case 24 fractions were obtain by using very small pressure increments between fractions to obtain highly monodisperse polymer. Only a small number of the fractions were analyzed for number-average and weight-average molecular weight and in each case the molecular weight distributions were near 1.2. The viscosity-average molecular weight was also obtained for some of the fractions. On the basis of a comparison of the polydispersities obtained with fractions 12, 14, 19, and 21, it is reasonable to assume that the other fractions will have comparable molecular weight distributions since the pressure increment between fractions was approximately the same (~10 bar). The parent polymer has a crystallinity of 36.8% and a polydispersity of 5.4. As shown in Table V, the percent crystallinity of the fractionated samples does not differ significantly from that of the parent, even though the dispersity of the fractions is reduced to 1.2. The melting temperature was 113 °C for the parent polymer as well as for the fractions.

Phase Behavior. As previously mentioned, the cloud-point curves described in this section are obtained at a fixed polymer concentration of ~5 wt %. Figure 4 shows that the P–T behavior of the PMA–F22 system is similar to that shown schematically in Figure 1B. In the fractionation experiments we found that the very high molecular weight oligomers in the parent polymer did not dissolve in F22 at pressures to 500 bar. Here we find that it is not possible to dissolve the high molecular weight parent polymer in F22 at temperatures of 100–150 °C even to pressures as high as 2000 bar, and therefore, we used fraction 6 (see Table II) for the cloud-point determinations. It is not surprising that higher pressures have little effect on the solubility behavior since the density of the Freon does not drastically change over the pressure range of 500–2000 bar. Propane at 150 °C and 2000 bar does not dissolve the parent polymer nor does it dissolve fraction 6. The vapor pressure for pure F22 is shown in Figure 4 as an indication of where the three-phase, LLV line would occur. At temperatures below ~90 °C the solution became very

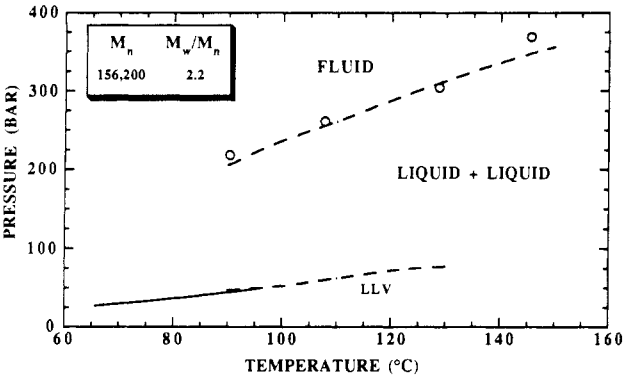

Figure 4. Cloud-point behavior of the poly(methyl acrylate)–chlorodifluoromethane system. The polymer concentration is 5.0 wt %. The dashed lines represent calculations with the Sanchez–Lacombe equation of state with k_{ij} = 0.005 and η_{ij} = −0.010. The solid line represents a portion of the vapor–liquid curve for pure chlorodifluoromethane.

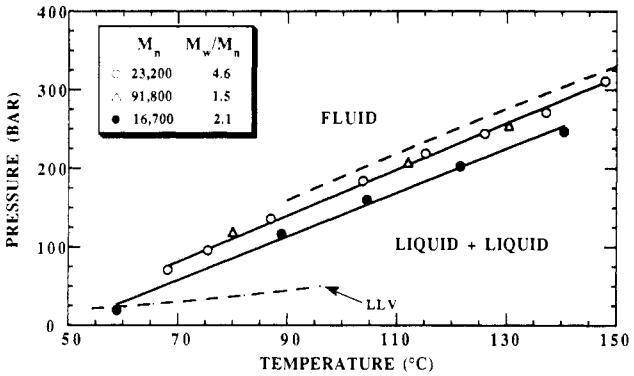

Figure 5. Cloud-point behavior of the (64 mol %/36 mol %) poly(ethylene-*co*-methyl acrylate)–chlorodifluoromethane system. The polymer concentration is 5.0 wt %. The solid lines are a linear fit of the experimental data. The dashed lines represent calculations with the Sanchez–Lacombe equation of state with k_{ij} = −0.125 and η_{ij} = −0.125.

viscous and it was not possible to obtain reliable cloud-point data. The data in Figure 4 show that modest pressures are needed to obtain a single phase at temperatures greater than 90 °C, which is consistent with the fractionation results which showed that the concentration of polymer in F22 increased quite rapidly at pressures above ~230 bar. The slope of the cloud-point curve, $[\partial P/\partial T]_x$ ~2.8 bar/K, is similar to those found with the polyisobutylene–hydrocarbon systems reported by Zeman and co-workers.[12]

Figure 5 shows the *P–T* behavior of the (64 mol %/36 mol %) EMA–F22 system. The molecular weight characteristics of the three copolymers shown in Figure 5 were determined with use of polyethylene standards (see Table IIIA). This system also exhibits the type of phase behavior shown schematically in Figure 1B. The cloud-point curves for this copolymer–F22 system not only have positive slopes with values similar to that found with the previously described PMA–F22 system, but they also occur in the same pressure range as the PMA–F22 system. Increasing the molecular weight of the copolymer from 16 700 to 91 800 causes only a small shift in the location of the cloud-point curves to higher pressures. A single, three-phase LLV point was obtained for the 16 700 M_n fraction. This point lies at the intersection of the projection of the cloud-point curve and the vapor pressure curve of pure F22, verifying that the vapor pressure curve for pure F22 gives a reasonable representation of the LLV line. It is interesting that the cloud-point curve of the parent copolymer with a number-average molecular weight of 23 200 and a molecular weight distribution of 4.6 is shifted

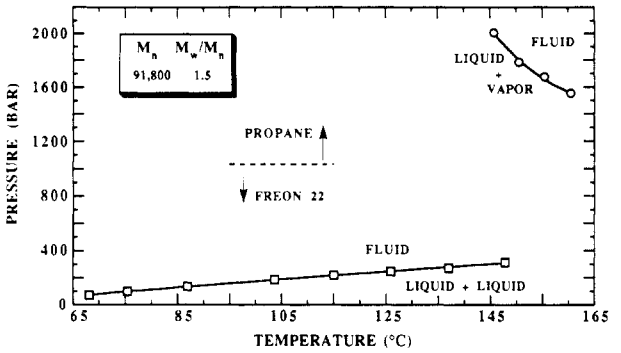

Figure 6. Comparison of the cloud-point behavior of poly(ethylene-*co*-methyl acrylate) (64 mol %/36 mol %) in chlorodifluoromethane and propane. The polymer concentration is 5.0 wt %. The line through the F22 data is a least-squares fit of the data. The line through the propane data represents calculations with the Sanchez–Lacombe equation of state with k_{ij} = 0.0235 and η_{ij} = −0.0015.

to higher pressures as compared to the curve for the fraction with a number-average molecular weight of 16 700 and a polydispersity of 2.1. The cloud-point curves of the parent copolymer and the fraction with a number-average molecular weight of 91 800 and a polydispersity of 1.5 are indistinguishable. Evidently the higher molecular weight species in the parent copolymer have a significant effect on the location of the cloud-point curve.

Figure 6 shows a comparison of the *P–T* behavior of poly(ethylene-*co*-methyl acrylate) (64 mol %/36 mol %) dissolved in propane and F22. The phase behavior for each of these two mixtures is radically different. As previously mentioned, the EMA–F22 system exhibits behavior similar to that shown in Figure 1A. However, the EMA–propane system exhibits the type of phase behavior shown in Figure 1D—that is, cloud-point pressures are essentially constant at high temperatures and they increase abruptly as the temperature is lowered. F22 is a much stronger solvent for the copolymer, probably because it hydrogen bonds to the acrylate groups in the backbone of the polymer. F22, at temperatures near 100 °C and pressures to 300 bar, is also more than twice as dense as propane at the same temperature and pressures to 2000 bar. The higher density of F22 facilitates the hydrogen-bonding and polar interactions with the copolymer even at temperatures as high as 150 °C, where F22 still exhibits a relatively high dielectric constant of ~4.[6] In the case of the propane–copolymer system, where the solvent is a nonpolar, non-hydrogen-bonding molecule, high temperatures are needed to reduce polymer–polymer interactions sufficiently to make the polymer accessible to the solvent. But, at these high temperatures, pressures as high as 2000 bar are needed to increase the density of propane to a high enough level to reduce the free-volume difference between the polymer and solvent and, thus, make the polymer soluble in propane.

Figure 7 shows the *P–T* behavior of poly(ethylene-*co*-methyl acrylate) (90 mol %/10 mol %) in propane. A crystallization boundary intrudes on the phase behavior in the vicinity of ~60 °C, otherwise the behavior shown schematically in Figure 1D would have occurred. Propane is such a good solvent for this copolymer that it depresses the melting temperature by about 25 °C ($T_{melt\text{-}90/10\ EMA}$ = 86 °C). The cloud-point curves in Figure 7 for this 10 mol % acrylate copolymer in propane are at much lower pressures than those for the previously described 36 mol % acrylate copolymer. Figure 7 shows that the cloud-point curves for two copolymers with approximately the same number-average molecular weight virtually superpose even though one copolymer has a molecular weight

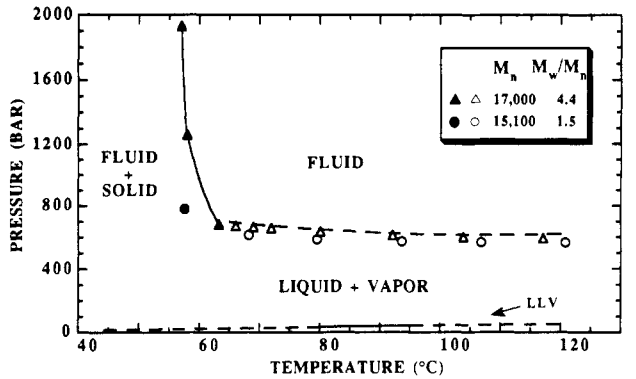

Figure 7. Cloud-point behavior of the (90 mol %/10 mol %) poly(ethylene-*co*-methyl acrylate)–propane system. The polymer concentration is 5.0 wt %. The solid symbols represent fluid → fluid + solid data and the open symbols represent fluid → liquid + vapor data. The dashed lines represent calculations with the Sanchez–Lacombe equation of state with η_{ij} fit to a function of temperature and $k_{ij} = 0$.

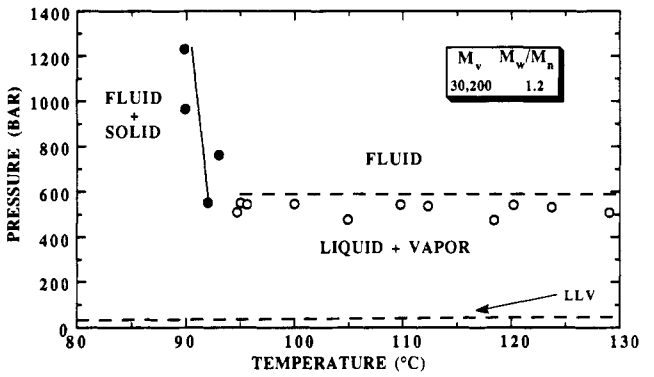

Figure 8. Cloud-point behavior of the branched polyethylene–propane system. The polymer concentration is 5.0 wt %. M_v is the viscosity-average molecular weight. The solid symbols represent fluid → fluid + solid data and the open symbols represent fluid → liquid + vapor data. The dashed lines represent calculations with the Sanchez–Lacombe equation of state with η_{ij} fit to a function of temperature and $k_{ij} = 0$.

distribution of 4.4 and the other has a distribution of 1.5. However, the cloud points for the copolymer with the lower polydispersity exhibited strong opalescence, indicating that its cloud-point curve is indeed very close to its critical mixture curve. The vapor pressure for pure propane is shown in Figure 7 as an indication of where the three-phase, LLV line would occur. Interestingly, F22 at temperatures of 100–150 °C and pressures up to 2000 bar cannot dissolve even a low molecular weight fraction (M_w = 22 600, M_n = 15 000) of this copolymer. The concentration of methyl acrylate groups in the backbone of the 90 mol %/10 mol % EMA is low enough that F22 is too polar to dissolve the copolymer even though it hydrogen bonds to the acrylate groups.

Figure 8 shows that the P–T behavior of the low-density polyethylene (PE)–propane system has the same characteristics as the (90 mol %/10 mol %) EMA–propane system. Both systems intersect a crystallization boundary at ~25 °C below the normal melting point of the polymers ($T_{melt\text{-}PE}$ = 113 °C; $T_{melt\text{-}90/10\ EMA}$ = 86 °C). Strong critical opalescence was observed for the cloud-point transitions of the polyethylene–propane system. The difference in location of the crystallization boundary is attributed to the difference in the crystallinity of the polymer, 38 versus 18%. The slight negative slope of the P–T trace of the cloud-point curve at high temperatures is similar to that found by Ehrlich and Kurpen[19] and Condo[20] for the polyethylene–propane system and Rätzsch, Findeisen, and Sernow[21] for the polyethylene–ethylene system. On the basis of our findings for the 90 mol %/10 mol % EMA–F22 system, it is not surprising that F22 does not dissolve even low molecular weight polyethylene.

Figures 4–8 show that as the concentration of polar repeat unit in the backbone of the polymer increases, the solvent characteristics needed to dissolve the polymer change dramatically. This change in solvent requirements is shown quite clearly in Figure 9, which compares the cloud-point curves for propane with three ethylene-based copolymers that have 100, 90, and 66 mol % ethylene. Although the molecular weight of the 66 mol %/34 mol % methyl acrylate copolymer is higher than that of the other two polymers, it is apparent that the conditions needed to dissolve the polymer change in a nonlinear fashion as the concentration of polar groups increases in the backbone of the polymer. Polymer composition has a greater effect on the phase behavior than does polydispersity. A similar nonlinear composition effect is observed with the F22–polymer mixtures shown in Figures 4 and 5. Although the acrylate content in the polymer is reduced from 100 to 34 mol %, there is little quantitative difference in the cloud-point behavior of these F22–polymer mixtures. However, when the acrylate content is reduced to 10 mol %, F22 does not dissolve the copolymer even at pressures to 2000 bar and temperatures to 160 °C. More work is in progress to measure the cloud-point behavior of poly(ethylene-*co*-methyl acrylate) polymers with acrylate contents between 10 and 34 mol % as well as to determine pure component polymer properties, such as dielectric constant, which should provide insight into the type of changes that occur with varying acrylate content.

Modeling

The objective of this section is to determine whether the Sanchez–Lacombe equation of state[5] can model the phase behavior exhibited by the polymer–solvent mixtures reported in this study. Although a mean-field equation of state does not directly account for hydrogen-bonding and polar interactions, we will show that it is possible to mimic the trends in the experimental data if the mixture parameters are allowed to vary with temperature as suggested by Sanchez and Balazs.[22]

The Sanchez–Lacombe equation of state is

$$\tilde{\rho}^2 + \tilde{P} + \tilde{T}\left[\ln(1-\tilde{\rho}) + \left(1-\frac{1}{r}\right)\tilde{\rho}\right] = 0 \qquad (1)$$

where $\tilde{T}, \tilde{P}, \tilde{v}$, and $\tilde{\rho}$ are the reduced temperature, pressure, volume, and density, respectively, that are defined as

$$\tilde{T} = T/T^* \qquad T^* = \epsilon^*/R \qquad (2)$$

$$\tilde{P} = P/P^* \qquad P^* = \epsilon^*/v^* \qquad (3)$$

$$\tilde{\rho} = 1/\tilde{v} = V^*/V \qquad V^* = N(rv^*) \qquad (4)$$

$$\rho^* = M/(rv^*) \qquad (5)$$

where ϵ^* is the mer–mer interaction energy, v^* is the close-packed molar volume of a mer, M is the molecular weight, N is the number of molecules, r is the number of sites (mers) a molecule occupies in the lattice, and R is the universal gas constant.

Characteristic parameters, T^*, P^*, and ρ^*, or equivalently, ϵ^*, v^*, and r, are needed for phase-equilibrium calculations. Table VI lists T^*, P^*, and ρ^*, the characteristic temperature, pressure, and close-packed mass density for the solvents and the homopolymers used in this study. The characteristic parameters for propane are obtained directly from Sanchez and Lacombe.[5] The parameters for F22 are determined in the following manner. ρ^* is given an initial value of 1.55 g/cm^3, which

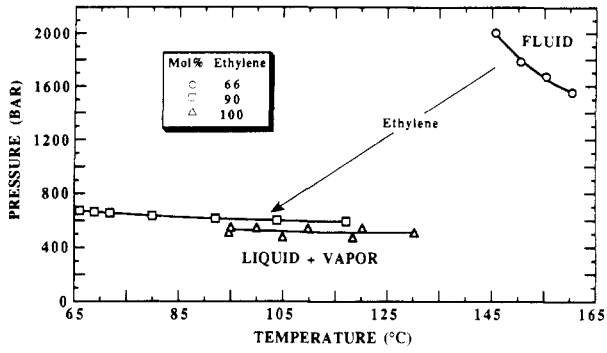

Figure 9. Effect of copolymer ethylene content on the cloud-point behavior of propane–polymer mixtures. The polymer concentration is 5.0 wt %.

Table VI
Characteristic Pure Component Parameters for the Solvents and Polymers Used in This Study

component	T^*, K	ρ^*, g/cm^3	P^*, bar
C_3H_8	371	0.690	3131
$CHClF_2$	351	1.666	4331
low-density polyethylene	671	0.887	3549
EMA[a] (90 mol %/10 mol %)	606	1.008	3760
EMA[a] (64 mol %/36 mol %)	510	1.208	4043
poly(methyl acrylate)	416	1.354	4272

[a] Poly(ethylene-*co*-methyl acrylate).

is 10% greater than the liquid density of F-22 at its normal boiling point. T^* and P^* are determined by fitting the equation of state to vapor–liquid equilibrium (VLE) data in the range of −40 to +66 °C. The difference between experimental and calculated saturation pressures is minimized while recording the difference between calculated and experimental liquid densities. The characteristic density is then changed and the procedure is repeated until the deviation between calculated and experimental saturation pressures is minimized. The predicted critical temperature and pressure, 95.7 °C and 48.4 bar, are very close to the actual values given in Table I. The average absolute deviation in the liquid molar volume along the portion of the VLE curve used to fit the parameters is 4.7% although the calculated critical density is low by ~30%.

Table VI shows the characteristic parameters for low-density polyethylene obtained from Sanchez and Lacombe.[5] In the case of poly(methyl acrylate), the characteristic parameters listed in Table VI are determined by using volumetric data obtained at temperatures ranging from 10 to 50 °C and at very low pressures.[23] Sanchez and Lacombe[24] suggested the use of the following equation to determine T^* and ρ^*.

$$T\alpha = 1/[\tilde{T}/(1-\tilde{\rho}) - 2] \tag{6}$$

where α, the thermal expansion coefficient, 6.49×10^{-4} °C^{-1}, is calculated from the data of Matheson et al.[23] The characteristic pressure, P^*, can be determined from the isothermal compressibility and the thermal expansion coefficient.[5] However, since data are not available on the isothermal compressibility, we determined P^* by equating it to the square of the Hildebrand solubility parameter, 10.1 (cal/cm^3)$^{0.5}$.[25]

Since there are no literature data on the pressure–volume–temperature properties of the two poly(ethylene-*co*-methyl acrylate) polymers, the characteristic parameters for these copolymers are calculated by the approach suggested by Panayiotou.[26] For these calculations, we assume that the copolymer is statistically random and that its characteristic parameters v^*, ϵ^*, and r can be described by the more general mixing rules given by Sanchez and Lacombe.[5] The characteristic volume of the copolymer, v_{co}^*, can be calculated by assuming pairwise additivity of the characteristic volumes of the two homopolymers which comprise the copolymer.

$$v_{co}^* = \sum_{A=1}^{2}\sum_{B=1}^{2}\phi_A\phi_B v_{AB}^* \tag{7}$$

with

$$v_{AB}^* = 0.5[(v_{AA}^* + v_{BB}^*)(1-\eta_{AB})] \tag{8}$$

where the subscripts A and B represent the two monomers in the copolymer, and the volume fractions, ϕ_A and ϕ_B are defined as

$$\phi_A = \frac{m_A}{\rho_A^* v_A^*} \Big/ \sum_{B=1}^{2}\left(\frac{m_B}{\rho_B^* v_B^*}\right) \tag{9}$$

where m_A is the mass fraction of component A in the copolymer and ρ_A^*, ρ_B^*, v_A^*, and v_B^* represent the characteristic parameters for homopolymers A and B. The characteristic interaction energy for the copolymer, ϵ_{co}^*, can be described by a van der Waals type mixing rule for the characteristic interaction energy between adjacent sites in a lattice.

$$\epsilon_{co}^* = \frac{1}{v_{co}^*}\sum_{A=1}^{2}\sum_{B=1}^{2}\phi_A\phi_B\epsilon_{AB}^* v_{AB}^* \tag{10}$$

with

$$\epsilon_{AB}^* = (\epsilon_{AA}^*\epsilon_{BB}^*)^{0.5}(1-k_{AB}) \tag{11}$$

where ϵ_{AA}^* and ϵ_{BB}^* represent the characteristic mer–mer interaction energies for homopolymers A and B. In principle, the two copolymer mixture parameters, k_{AB} and η_{AB}, are used to account for specific interactions between the two homopolymers, A and B, which comprise the copolymer. However, these parameters will be set equal to zero since they had little effect on the calculated phase behavior. It should be noted that Panayiotou[26] found that nonzero values of k_{AB} and η_{AB} had a large effect on the phase behavior of copolymer–copolymer and copolymer–homopolymer mixtures.

The mixing rule for the number of sites a pure copolymer occupies, r_{co}, is given by

$$1/r_{co} = \sum_{B=1}^{2}(\phi_B/r_B) \tag{12}$$

where r_B represents the characteristic parameters for homopolymers A and B.

The mixing rules used to calculate the phase behavior of polymer–solvent mixtures are identical in form to eqs 7–12 except that instead of summing over the two components found in a copolymer, the sum is over the two components in the polymer–solvent mixture. Also, the mixture parameters in eqs 8 and 11 are polymer–solvent interaction parameters rather than homopolymer–homopolymer interaction parameters. By use of the methods described by Sanchez[27] the chemical potential of a component in a mixture, μ_i, is derived as

$$\mu_i = RT\left[\ln\phi_i + \left(1-\frac{r_i}{r}\right)\right] + r_i\left\{-\tilde{\rho}\left[\frac{2}{v^*}\left(\sum_{j=1}^{c}\phi_j v_{ij}^*\epsilon_{ij}^* - \epsilon^*\sum_{j=1}^{c}\phi_j v_{ij}^*\right) + \epsilon^*\right] + RT\tilde{v}\left[(1-\tilde{\rho})\ln(1-\tilde{\rho}) + \frac{\tilde{\rho}}{r_i}\ln\tilde{\rho}\right] + P\tilde{v}\left(2\sum_{j=1}^{c}\phi_j v_{ij}^* - v^*\right)\right\} \tag{13}$$

At equilibrium, the chemical potential of the components present in each of the phases must be equal. For the ethylene-rich polymers that crystallize, we make no attempt to determine the pressure–temperature trace of the crystallization boundary. If the polymer fractions were truly "monodisperse", the cloud point would be the intersection of the pressure–composition (P–x) isotherm at an overall polymer concentration of 5 wt %.[29-31] Since the equation of state does not account for hydrogen bonding and, even with temperature-dependent parameters, it does only a fair job accounting for polar interactions, we will use the cloud points calculated at 5 wt % polymer in solution, ignoring the molecular weight distributions. The pressure–temperature (P–T) trace of the cloud-point curve is obtained by calculating P–x isotherms to temperatures as low as the crystallization boundary. The P–T trace of the liquid–liquid–vapor line is also obtained from the P–x isotherms.

The dashed line in Figure 4 shows the fit of the Sanchez–Lacombe equation of state to the cloud-point curve for the PMA–F22 system with k_{ij} = 0.005 and η_{ij} = –0.010. With the two mixture parameters set equal to zero, a reasonable estimate of the cloud-point curve is obtained. However, to obtain a more quantitative representation of the cloud-point curve over the entire temperature range, a negative value for η_{ij} is needed as well as a small positive value of k_{ij}. The cloud-point curve shifts to higher pressures but maintains the same slope with increasing values of k_{ij} while holding η_{ij} constant. Changing η_{ij} affects the slope of the cloud-point curve. It is a bit surprising that a positive value of k_{ij} is needed since F22 is expected to exhibit specific interactions with PMA (i.e., hydrogen bonding), which should result in a larger mixing interaction energy, ϵ^*, usually accounted for with a negative value for k_{ij}.[28] The calculated LLV line superposes on the pure component vapor pressure curve of F22 and it extends to higher temperatures.

The dashed line in Figure 5 shows the fit of the Sanchez–Lacombe equation to the cloud-point curve for the (64 mol %/36 mol %) EMA–F22 system with k_{ij} = –0.125 and η_{ij} = –0.125. Even with larger negative values of the mixture parameters, it is not possible to obtain a better fit of the cloud-point data. More positive values of k_{ij} shift the cloud-point curve to higher pressures while maintaining the same slope. However, as with the PMA–F22 case, changing the value of η_{ij} changes the slope of the cloud-point curve. Although the experimentally observed phase behavior of the (64 mol %/36 mol %) EMA–F22 and the PMA–F22 systems are very similar, the mixture parameters needed to represent the behavior are significantly different probably due either to an inherent limitation in the equation of state to account for nonrandom mixing found for these hydrogen-bonding systems or to the mixing rules chosen to determine the characteristic parameters for EMA. For the calculations presented in Figure 5, nonzero values for the copolymer interaction parameters, k_{AB} and η_{AB}, have only a minor effect on the calculated cloud-point curve, and therefore, these parameters are set equal to zero. As shown in Figure 5, the calculated LLV line superposes on the pure component vapor pressure curve of F22 and it extends to temperatures higher than the critical temperature of F22.

Figure 6 shows a comparison of the cloud-point behavior of 64 mol %/36 mol % EMA in F22 and propane. The line through the propane data is a best fit of the Sanchez–Lacombe equation with k_{ij} = 0.0235 and η_{ij} = –0.0015. If k_{ij} becomes more positive the curve shifts to higher pressures, and if η_{ij} becomes more positive the curve shifts to lower pressures. However, the shift in the curve and its slope are more sensitive to changes in η_{ij} than k_{ij}. Again, nonzero values for the copolymer interaction parameters, k_{AB} and η_{AB}, have only a minor effect on the location of the calculated cloud-point curve so they are set equal to zero.

The fit of the (90 mol %/10 mol%) EMA–propane system is shown as a dashed line in Figure 7. We expect k_{ij} to be close to zero since the bulk of i–j interactions in solution are between propane and ethylene segments, which should be similar in strength to that of propane–propane and ethylene–ethylene interactions. If η_{ij} is set equal to zero and k_{ij} is allowed to vary with temperature, we can get a reasonable fit of the cloud-point data, but the calculated curve would be strictly empirical since k_{ij} should be close to zero, based on the molecular arguments just mentioned. If both k_{ij} and η_{ij} are set equal to zero, the calculated cloud-point curve has a positive slope and, therefore, is not even qualitatively similar to that observed experimentally. The fit of the cloud-point curve up to the crystallization boundary shown in Figure 7 is obtained by setting k_{ij} equal to zero and allowing η_{ij} to vary linearly with temperature as given in eq 14. It is possible to obtain

$$\eta_{ij} = 0.052 - 0.001T\ (°C) \tag{14}$$

a slightly better fit of the data with k_{ij} = –0.008, but the scatter in the data associated with polymer cloud-point measurements does not warrant using a nonzero value for k_{ij}. η_{ij} becomes more negative as the temperature increases, suggesting that the close-packed molar volume of an i–j pair occupies a larger volume than the arithmetic average of the two volumes. The temperature variation in η_{ij} can be ascribed to the differences in the free volume between the polymer and solvent. At high temperatures, where η_{ij} is more negative, this difference should be large as the solvent expands more rapidly than the polymer. Although an alternative approach to modeling the cloud-point behavior in Figure 7 is to account for the thermal expansion of propane by fitting its characteristic parameters to functions of temperature, this approach still requires a temperature-dependent η_{ij} to fit the data and therefore was not used.

The fit of the cloud-point curve for the polyethylene–propane system up to the crystallization boundary is shown in Figure 8 as a dashed line. Using the arguments given in the previous paragraph, k_{ij} is set equal to zero and η_{ij} is given by eq 15. It is interesting that the temperature

$$\eta_{ij} = 0.074 - 0.002T\ (°C) \tag{15}$$

dependence of η_{ij} is more pronounced for the polyethylene–propane system, where the crystallinity of polymer is ~38%, than for the (90 mol %/10 mol %) EMA–propane system, where the crystallinity of the copolymer is ~18%, suggesting that the differences in free volume between polymer and solvent increase with polymer crystallinity. As with the previous system, the calculated cloud-point curve exhibits a positive slope if k_{ij} and η_{ij} are set equal to zero. We again found that even if the characteristic parameters of both propane and polyethylene are fit to functions of temperature to account for thermal expansion, it was still necessary to use a temperature-dependent η_{ij} to fit the data, and therefore, this approach was not used.

A number of trends can be seen in the modeling results of the propane–polymer systems shown in Figures 6–8. For the mixtures of propane with the high ethylene content polymers, 100, 90, and 66 mol %, we find that values of k_{ij} were zero, or small and positive, as expected from molecular arguments concerning the types of interactions occurring between propane and ethylene segments. Interestingly, the value for the other mixture parameter, η_{ij}

is large and negative for the most crystalline polymer and it becomes less negative as the crystallinity decreases. Also, it is necessary to make η_{ij} a function of temperature for the two most crystalline polymers investigated in this study. The variation of η_{ij} with temperature or polymer crystallinity is attributed to the free-volume differences between the solvent and polymer. It should be noted that the temperature dependence of η_{ij} cannot be eliminated if the pure component parameters of both propane and the polymer are made functions of temperature.

The trends in the modeling results of the chlorodifluoromethane–polymer systems shown in Figures 4 and 5 are less obvious. On the basis of molecular arguments we expected k_{ij} to vary with temperature[28] and acrylate content. However, this was not the case for the poly(methyl acrylate) and 90 mol %10 mol % EMA systems. Perhaps it should not be surprising that a mean-field equation of state with combining rules that assume random mixing does not do a good job modeling mixtures that exhibit specific, non-mean-field interactions, and nonrandom mixing.

Conclusions

The properties of a solvent needed to dissolve poly(ethylene-*co*-methyl acrylate) change dramatically with acrylate content. As the methyl acrylate content increases from 0 to only 34 mol %, the copolymer becomes virtually insoluble in nonpolar propane, but becomes readily soluble in F22, which is polar and can hydrogen bond. This nonlinear chemical composition effect has a stronger influence on the phase behavior than does polydispersity. Comparing the ability of F22 to readily solubilize high acrylate content copolymers, with the inability of propane to dissolve these copolymers, suggests that hydrogen bonding between the Freon and the basic acrylate group in the copolymer dominates polymer–solvent dispersion and polar interactions. For the high ethylene content polymers, which are readily dissolved in propane compared to F22, dispersion forces are the dominant mode of interaction in solution. Although Freon and propane have similar polarizabilities, Freon has a large dipole moment, which makes it too polar to dissolve nonpolar ethylene-rich polymers.

One difficulty in modeling copolymer–solvent phase behavior is that very little pure component copolymer data exist that can be used to determine characteristic parameters. The nonlinear effect of chemical composition in the backbone of the copolymer on the phase behavior suggests that it is not a straightforward task to derive appropriate mixing rules to calculate copolymer characteristic parameters solely from homopolymer data. In addition, contemporary polymer solution equations of state, such as the Sanchez–Lacombe equation used in this study, do not account for the nonrandom mixtures that occur with hydrogen-bonded systems. It is very difficult to ascertain, as well as interpret, the trends in the values of the mixture parameters obtained as a function of copolymer composition. A larger copolymer–solvent data base is needed before these trends can even be correlated.

Acknowledgment. We thank Sang-Ho Lee, who helped with the phase equilibrium experiments, Professor Dwaine O. Cowan at Johns Hopkins University, who allowed us to use his differential scanning calorimeter, and Professor Donald Paul at the University of Texas, for helpful technical discussions on the phase behavior of polyethylene–solvent systems. We also thank Michael F. Franckowiak and Walter J. Krug who designed and built the view cell, which operates to 2000 bar. We thank the National Science Foundation for partial support of this project under Grant EET-88-15629.

References and Notes

(1) Baron, N. A new polyolefin product family based on Exxpol catalyst technology. Presented at the 2nd International Symposium on High Pressure Chemical Engineering, Erlangen, Germany, September 1990.
(2) Rätzsch, M. T.; Wagner, P.; Wohlfarth, Ch.; Heise, D. *Acta Polym.* **1982**, *33*, 463.
(3) Rätzsch, M. T.; Wagner, P.; Wohlfarth, Ch.; Gleditzsch, S. *Acta Polym.* **1983**, *34*, 340.
(4) Wohlfarth, Ch.; Wagner, P.; Rätzsch, M. T.; Westmeier, S. *Acta Polym.* **1982**, *33*, 468.
(5) Sanchez, I. C.; Lacombe, R. H. *Macromolecules* **1978**, *11*, 1145.
(6) Uematsu, M.; Franck, E. U. *Ber. Bunsenges. Phys. Chem.* **1989**, *93*, 177.
(7) Izatt, R. M.; Schofield, R. S.; Faux, P. W.; Harding, P. R.; Christensen, S. P.; Christensen, J. J. *Thermochim. Acta* **1983**, *68*, 223.
(8) Scott, R. L.; van Konynenburg, P. H. *Discuss. Faraday Soc.* **1970**, *49*, 87.
(9) McHugh, M. A.; Krukonis, V. J. *Supercritical Fluid Extraction: Principles and Practice*; Butterworths: Boston, MA, 1986.
(10) Allen, G.; Baker, C. H. *Polymer* **1965**, *6*, 181.
(11) Baker, C. H.; Clemson, C. S.; Allen, G. *Polymer* **1966**, *7*, 525.
(12) Zeman, L.; Biros, J.; Delmas, G.; Patterson, D. *J. Phys. Chem.* **1972**, *76*, 1206.
(13) Seckner, A. J.; McClellan, A. K.; McHugh, M. A. *AIChE J.* **1988**, *34*, 9.
(14) Irani, C. A.; Cosewith, C. *J. Appl. Polym. Sci.* **1986**, *31*, 1879.
(15) Krukonis, V. J.; Kurnik, R. T. *J. Chem. Eng. Data* **1985**, *30*, 247.
(16) Watkins, J. J.; Krukonis, V. J.; Condo, P. D.; Ehrlich, P. Fractionation of high density polyethylene with supercritical propane at temperatures above and below the second critical end point. Presented at the AIChE Spring National Meeting, Orlando, FL, 1990.
(17) McHugh, M. A.; Guckes, T. L. *Macromolecules* **1985**, *18*, 674.
(18) Diguet, R.; Deul, R.; Franck, E. U. *Ber. Bunsenges. Phys. Chem.* **1987**, *91*, 551.
(19) Ehrlich, P.; Kurpen, J. J. *J. Polym. Sci. Part A* **1963**, *1*, 3217.
(20) Condo, P. D. Fractionation of polyethylene in *n*-propane: solid–fluid and liquid–gas equilibria at 110 °C to 140 °C and to 750 bar. M.S. Thesis, State University of New York at Buffalo, 1989.
(21) Rätzsch, M. T.; Findeisen, R.; Sernow, V. S. *Z. Phys. Chem.* **1980**, *261*, 995.
(22) Sanchez, I. C.; Balazs, A. C. *Macromolecules* **1989**, *22*, 2325.
(23) Matheson, M. S.; Auer, E. E.; Bevilacqua, E. B.; Hart, E. J. *J. Am. Chem. Soc.* **1951**, *73*, 5395.
(24) Sanchez, I. C.; Lacombe, R. H. *Polym. Lett.* **1977**, *15*, 71.
(25) Askadskii, A. A.; Kolmakova, L. K.; Tager, A. A.; Slonimskii, G. L.; Korshak, V. V. *Dokl. Phys. Chem. (Engl. Transl.)* **1976**, *226*, 99.
(26) Panayiotou, C. G. *Makromol. Chem.* **1987**, *188*, 2733.
(27) Sanchez, I. C. *Macromol. Sci.-Phys.* **1980**, *B17*, 565.
(28) Reid, R. C.; Prausnitz, J. M.; Polling, B. E. *The Properties of Gases and Liquids*, 4th ed.; McGraw-Hill: New York, 1987.
(29) Koningsveld, R.; Staverman, A. J. *J. Polym. Sci., Part A-2* **1968**, *6*, 305.
(30) Koningsveld, R.; Staverman, A. J. *J. Polym. Sci., Part A-2* **1968**, *6*, 325.
(31) Koningsveld, R.; Staverman, A. J. *J. Polym. Sci., Part A-2* **1968**, *6*, 349.

Registry No. Poly(methyl acrylate), 9003-21-8; chlorodifluoromethane, 75-45-6; poly(ethylene-*co*-methyl acrylate), 25103-74-6; polyethylene, 9002-88-4; propane, 74-98-6.